First-order vortex phase transition in $Bi_2Sr_2CaCu_2O_y$ single crystals with different carrier concentrations studied by resistivity measurements

S. Watauchi,* H. Ikuta,† H. Kobayashi, J. Shimoyama, and K. Kishio
Department of Superconductivity, The University of Tokyo, Hongo 7-3-1, Bunkyo-ku, Tokyo 113-8656, Japan
(Received 2 December 2000; published 24 July 2001)

The first-order vortex phase transition (FOT) in $Bi_2Sr_2CaCu_2O_y$ single crystals with different carrier concentrations was investigated by measuring the in-plane resistivity (ρ_{ab}) under a magnetic field applied parallel to the crystallographic *c*-axis direction. With a decrease in the temperature, ρ_{ab} dropped sharply at the FOT temperature when the applied field was smaller than the second-peak field (H_{pk}) that was determined by measuring the magnetic hysteresis curves at 25–30 K, while no such abrupt change was observed when the applied field was larger than H_{pk}. The temperature range where the FOT was observed was approximately between 0.6 to 0.95 in the scale of the reduced temperature ($t=T/T_c$) for all crystals. The first-order transition field (H_t) as a function of t shifted to higher fields as the carrier concentration of the crystal increased, which can be well scaled by the electromagnetic anisotropy factor (γ). Irrespective of the carrier doping level, the temperature dependence of H_t is experimentally expressed better by $H_t \propto (t^{-1}-t)$ rather than the functional form proposed by the conventional decoupling theory of the vortex lattice $[H_t \propto (t^{-1}-1)]$. This experimental formula can be accounted for by the decoupling theory if the temperature dependence of the magnetic penetration depth is assumed to scale as $\lambda^{-2} \propto (1-t^2)$.

DOI: 10.1103/PhysRevB.64.064520 PACS number(s): 74.60.Ec, 74.72.Hs, 74.25.Fy

I. INTRODUCTION

It is well established by now that the mixed state of high-temperature superconductors (HTSC) is rich in new physics, and its study is currently one of the most active areas in HTSC research. Theoretically, many novel concepts and ideas have been proposed, such as the vortex lattice melting transition,[1] the vortex glass transition,[2] and the decoupling transition.[3] Experimentally, the earliest clear evidence of the first-order vortex phase transition (FOT) was found in the resistivity data of $YBa_2Cu_3O_y$ (YBCO) single crystals.[4] The first thermodynamical support for the existence of the FOT was reported by Zeldov *et al.*[5] who observed a discontinuous step in the local magnetic flux density across the transition in a $Bi_2Sr_2CaCu_2O_y$ (Bi2212) single crystal. Subsequently, the observation of discontinuous jumps in magnetization was reported for YBCO,[6] and simultaneous measurements of resistivity and magnetization of YBCO revealed that the locations of the magnetization jumps in the *H-T* plane coincide with those of the resistive drops.[7] We observed similar drops in the temperature dependence of the in-plane resistivity (ρ_{ab}) of Bi2212, and confirmed that they are well correlated with the discontinuous steps of magnetization.[8] Through these studies, the concept of the FOT was experimentally well established. The FOT was also studied by calorimetric measurements in YBCO,[9] and the existence of the FOT was reported for $(La_{1-x}Sr_x)_2CuO_4$ (LSCO) (Refs. 10 and 11) as well. As for the nature of the FOT, the results of a multiterminal transport measurement on Bi2212 was interpreted as a simultaneous melting and decoupling (a sublimation scenario),[12] while another group asserted that melting and decoupling transitions occur separately based on a similar measurement.[13]

Recently, a universal behavior of the temperature dependence of the FOT was reported[11] for several HTSC's with quite different values of the electromagnetic anisotropy parameter ($\gamma^2 \equiv m_c^*/m_{ab}^*$). The scaling parameters were γ^2 and the spacing between the superconducting planes (s). This result clearly shows the importance of the anisotropy in describing the nature of the FOT. In Bi2212 single crystals, the anisotropy is controllable by changing the oxygen content.[14] Therefore, it is very interesting to study the FOT in Bi2212 single crystals with various oxygen content. However, there are still only rather limited numbers of published works[15,16] concerning the vortex phase transition, in which the carrier concentration was systematically controlled. Moreover, the earlier systematic works are restricted to magnetization measurements. Resistivity, which is complemental to magnetization, has been studied in crystals, for which the carrier concentration was not intentionally varied.[8,17]

In the present study, we measured ρ_{ab} of Bi2212 single crystals in which the carrier concentration was carefully and systematically controlled. We investigate the temperature dependence as well as the carrier concentration dependence of the FOT fields in these crystals. Comparisons between the experimental results and the predictions of some theories[1,3] are made, in which we take the temperature dependence of the magnetic penetration depth (λ) into account. As a result, we observed clear resistivity drops due to the FOT in all crystals with different carrier doping states. The FOT fields (H_t) in these crystals as a function of reduced temperature ($t=T/T_c$) shifted to higher field with reducing the anisotropy and H_t was scaled well with γ^2. The behavior of the FOT in these crystals was approximately consistent with the conventional decoupling theory,[3] which predicts $H_t \propto (t^{-1}-1)$. We found, however, $H_t \propto (t^{-1}-t)$ better fits to the experimental results. This latter relation can be derived from the decoupling theory by supposing that the temperature dependence of λ is experimentally expressed by $\lambda^{-2} \propto (1-t^2)$ (Ref. 18) rather than by the two-fluid formula near T_c, $\lambda^{-2} \propto (1-t)$.

II. EXPERIMENTAL

Single crystals of Bi2212 were grown by the floating-zone (FZ) technique.[19] Bi_2O_3, $SrCO_3$, $CaCO_3$, CuO powders (99.9%) with a nominal composition of $Bi_{2.1}Sr_{1.8}CaCu_2O_y$ were mixed with ethanol. The powder mixture was well dried and put into a container made of silver foil. The mixture was calcined in air at 770 °C for 24 h and pulverized well after the calcination. Single phase powder of Bi2212 was obtained after the second calcination in air at 840 °C for 48 h. To form a cylindrical rod with a dimension of approximately 7 mm $\phi \times 120$ mm, the powder was then put into a long thin-wall rubber tube and was pressed with a pressure of 10^3 kg/cm^2. The obtained rods were sintered in air at 850 °C for 5 h.

The crystals were grown using an infrared heating furnace equipped with two ellipsoidal mirrors and two halogen lamps as heat sources (Nichiden Machinery Ltd. Model No. SC15-HD). As a sintered rod is rather porous, a zone pass was first performed with a velocity of 60 mm/h in an oxygen gas-flowing atmosphere to enhance the density of the rod. The typical size of a zone-passed rod was about 6 mm $\phi \times 100$ mm. Crystal growth was made in the 1 atm oxygen-flowing condition using a zone-passed rod. An as-prepared zone-passed rod was used as a feed rod and a conically shaped rod as a seed rod. First, the end of the feed rod was put into the heating zone of the infrared furnace and was melted. Thereafter, the distance between the feed and the seed rods was gradually reduced to form a molten zone. During the zone melting, the two rods were rotated in counter directions at about 25 rpm. During the first few hours after seeding, the seed rod was moved substantially faster than the feed rod to make necking. Then the velocity of both rods were gradually changed to make the molten region thicker. In the stabilized state, feed and seed velocities were set to 0.20 and 0.25 mm/h, respectively.

The typical size of the grown crystal rod was 5 mm $\phi \times 100$ mm. The chemical composition of the grown rod was analyzed by the inductively-coupled-plasma (ICP) technique and found to be $Bi_{2.2_2}Sr_{1.6_2}Ca_{1.0_1}Cu_2O_y$. After cutting and cleaving the grown rod, thin plate-shaped single crystals of Bi2212 were obtained, the largest size of which was approximately $10 \times 5 \times 0.1$ mm^3. To release thermal strains which were introduced during the crystal growth, as-grown crystals were annealed at 800 °C for three days in air and quenched to room temperature. Annealed crystals were then cut and cleaved into a platelike shape, typically $3 \times 0.4 \times 0.015$ mm^3 in dimension. The electrodes for resistivity measurements were prepared on the fresh surface using gold paste. Gold paste was painted in the four-terminal configuration for the in-plane resistivity measurement, and was heated at 800 °C for 1 h.

For the resistivity measurements, contacts to the gold pads on the crystals were made using gold wires and silver paste. Typical contact resistance was about 1 Ω. Resistivity was measured by a four-probe method using an ac resistance bridge (Linear Research LR-700). The frequency of the ac current was 16 Hz. Usually, the integration time of the resistance bridge was set to 1 s and resistivity was measured by sweeping the temperature continuously with a rate of 10–15 K/h. However, in the temperature range where the resistivity was less than 10^{-7} Ω cm, the temperature was kept constant at each data point, and the measurement was performed with an integration time of 10 s. The ac current was set to either 3 or 10 mA, corresponding to 50–150 A/cm^2 in current density depending on the size of the crystal. The magnetic field was always applied parallel to the *c*-axis direction of the crystals. The superconducting critical temperature (T_c) of the crystals was determined from the ρ_{ab}-T curves under zero magnetic field with a criterion of $\rho_{ab} = 10^{-10}$ Ω cm.

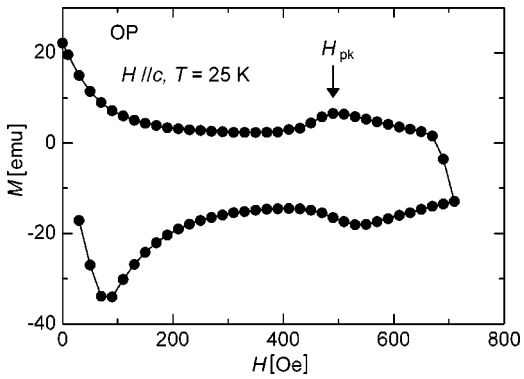

FIG. 1. The magnetic hysteresis loop of crystal OP at 25 K. The arrow in the figure indicates how H_{pk} is determined.

To vary the carrier doping state from the underdoped state to the overdoped state systematically, the crystals were sealed in quartz tubes under controlled oxygen pressures [1.3×10^{-4} atm for crystal UN (underdoped), 1.3×10^{-3} atm for crystal OP (optimally doped), and 0.94 atm for crystals OV1–OV6 (overdoped) at room temperature] after the electrodes were prepared using gold paste. Except crystal UN, the sealed crystals were annealed at 450 °C for one day and at 400 °C for two days. Crystal UN was annealed at 600 °C for 12 h. After annealing, the quartz tube was quenched into iced water. The doping states of the crystals were characterized by T_c and the magnetically observed second peak field (H_{pk}) which was determined by measuring the magnetic hysteresis curves at 25–30 K. The value of H_{pk} is known to correlate well with the doping state in Bi2212.[20] The magnetic hysteresis loops were measured using a superconducting quantum interference device (SQUID) magnetometer (HOXAN HSM-2000X).

III. RESULTS

A typical result of magnetic hysteresis measurements is shown in Fig. 1, which indicates how the second peak field H_{pk} was determined. The origin of this second peak effect is still not quite understood, but it is in general accepted that it is related to a transition from a phase with a quasi-long-translational order to a state with no topological order at high fields.[21–24] Experimentally, the second peak field varies with the carrier density,[20,25] which we interpret that H_{pk} depends on the anisotropy. Some of the theories relate H_{pk} to the anisotropy factor γ. While the perhaps more realistic Bragg-

TABLE I. The values of T_c, H_{pk}, γ and the annealing conditions of the crystals used in this study.

Sample	T_c (K)	H_{pk}(Oe)	γ
UN[a]	78.3	200	209
OP	84.2	490	133
OV1	78.5	780	105
OV2[b]	78.3[b]	820	103
OV3	77.1	870	100
OV4[c]	76.4	910	98
OV5[c]	76.7	920	97
OV6[d]	75.2	1050[d]	91

[a]The annealing temperature of crystal UN was 600 °C, while the annealing time was limited to 12 h to preserve the electrodes from damage.

[b]T_c of crystal OV2 was determined by measuring the temperature dependence of dc magnetization under a magnetic field of about 1 Oe using a SQUID magnetometer, while for the other crystals, T_c was determined from the resistivity measurements in zero magnetic field. The data of crystal OV2 was reported previously (Ref. 8).

[c]The resistivity data of OV4 and OV5 were measured by using a resistance option (P4000) attached to a Quantum Design Physical Property Measurement System (PPMS) Model 6000 (Quantum Design). The resistance bridge method used for the other crystals had about one and a half order better sensitivity than the PPMS system.

[d]Crystal OV6 is significantly heavier doped than crystals OV1–OV5, as is evident from the values of T_c and H_{pk}, although the same annealing condition was adopted. This is probably because crystal OV6 was taken from a different rod. For this particular sample, the value of H_{pk} was not determined by measuring the same crystal, but a different crystal that was annealed in the same quartz tube.

to-vortex glass transition model involves some indeterminable parameters, such as H_{c2} in the expression of the transition field,[22] that in the dimensional crossover model[26] is simply given by

$$H_{3D\text{-}2D} \sim \frac{\Phi_0}{\gamma^2 s^2}, \tag{1}$$

where Φ_0 is the flux quantum and s is the spacing between the superconducting planes. In our previous studies, we estimated the anisotropy factor of Bi2212 according to Eq. (1), but encountered no difficulty in the interpretation of the data.[11,20] Furthermore, in the Bragg-to-vortex glass transition theory, the transition may coincide with the decoupling transition in a very anisotropic system like Bi2212.[22] For these reasons, we use the γ values estimated using Eq. (1) in this paper.

Table I gives a summary of the values of T_c, H_{pk}, and γ of the crystals studied in the present work, and Fig. 2 plots T_c as a function of γ. This plot corresponds to the well-known bell-shape behavior of T_c as a function of carrier concentration, where γ systematically decreases as the carrier concentration increases.[14] Judging from the behavior of

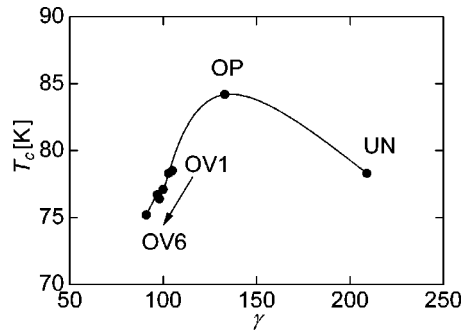

FIG. 2. T_c of the crystals used in this work as a function of γ.

T_c shown in Fig. 2, the doping states of the crystals listed in Table I are underdoped (UN), optimally doped (OP), and overdoped (OV1–OV6), respectively. Although the annealing of crystals was performed with a very similar condition for OV1–OV6, a slight difference in the partial pressure of oxygen was unavoidable. As a result, there is a variation of T_c and γ, showing how Bi2212 is sensitive to the annealing atmosphere. The carrier concentration of crystals OV1–OV6 gradually increases from a slightly overdoped state of OV1 to a heavily overdoped state of OV6. Note that T_c and γ are varying consistently even in this small range of T_c, supporting that H_{pk} is a good measure of the anisotropy.

Figure 3 shows the ρ_{ab}-T curves of UN, OP, and OV6. The magnitude of ρ_{ab} in the normal states ($\sim$90 K) decreased from roughly 10^{-3} Ω cm in UN to 10^{-4} Ω cm in OV6 with the increase in the carrier concentration. This behavior is consistent with previously published data.[14] It is evident that ρ_{ab} sharply drops with temperature decreasing near the tail of each ρ_{ab}-T curve when the applied field is smaller than H_{pk} of the respective crystal. This resistivity drop corresponds to the FOT.[8] The resistivity value at the on-set of FOT ranged approximately between 10^{-10} and 10^{-8} Ω cm. The arrows in Fig. 3(a) indicate how the FOT temperature (T_t) and T_c were defined in this study. The data of OV2 were reported previously, and it was found that the temperature of the drop in the resistivity coincides well with that of a discontinuous jump in magnetization of the same crystal.[8] The consistency of T_t between resistivity and magnetization measurements were also confirmed for OP, OV1, and OV3 in the present study. On the other hand, when the applied field exceeded H_{pk} of the crystal, ρ_{ab}-T curves became broadened without any noticeable structure, except of a small field range for OV6. The second peak field of OV6 exhibited a slight temperature dependence, while it depended only weakly on temperature for crystals with a lower carrier density. This behavior is consistent with the data reported in the literatures,[25,27] and the critical point where the FOT disappeared was somewhat larger in the field than H_{pk} which was determined at 30 K.

OV1–OV5 were annealed with the identical condition, and the doping state judged from T_c and γ is almost the same. Nevertheless, the detailed behavior of the ρ_{ab}-T curves was not the same. Figure 4 shows the resistivity curves for three of these crystals measured with the same applied field. OV2 has larger resistivity and a significantly broader vortex phase transition when compared with the

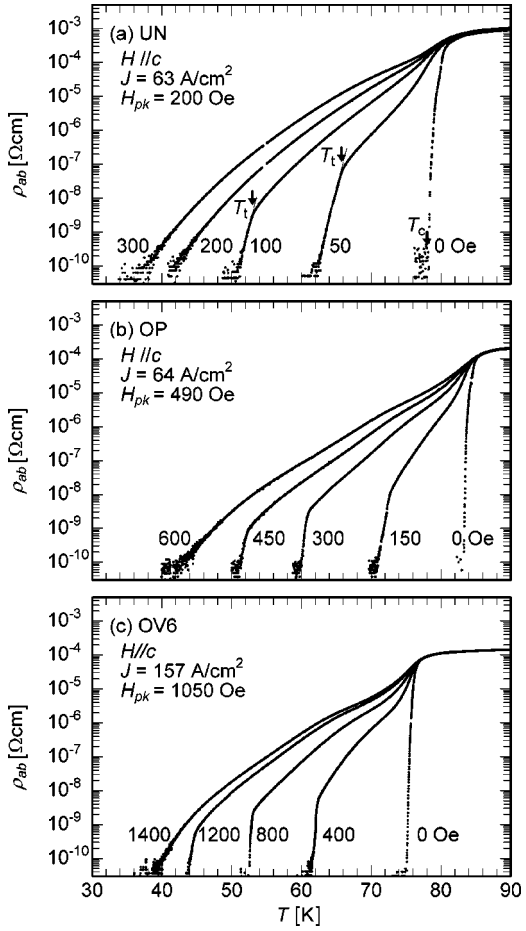

FIG. 3. Temperature dependencies of resistivity of crystals UN (a), OP (b), and OV6 (c). T_c and the FOT temperature (T_t) were defined as indicated in (a).

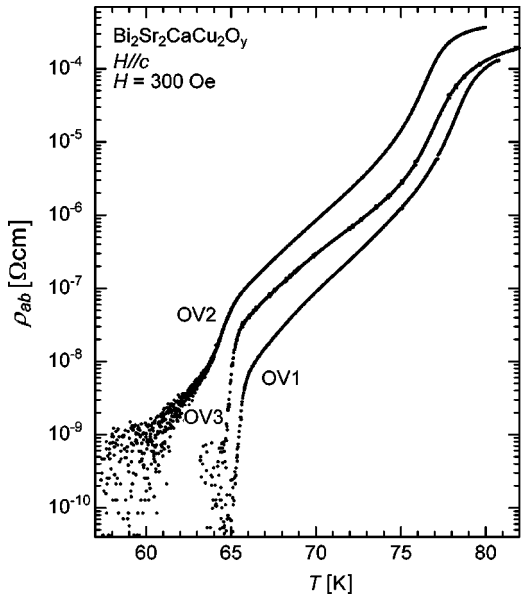

FIG. 4. Temperature dependence of the resistivity of crystals OV1, OV2, and OV3 at 300 Oe.

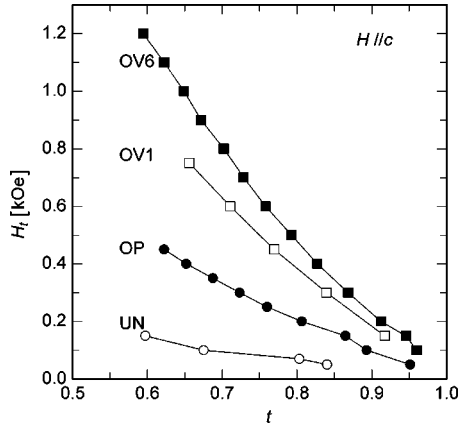

FIG. 5. The FOT fields of some of the Bi2212 crystals studied in the present work plotted as a function of the reduced temperature ($t=T/T_c$). As the carrier concentration of the crystal increases, the phase boundary shifts to higher field.

other two crystals. These differences in the behavior of ρ_{ab}-T could be attributed to the effect of impurities. Very interestingly, however, the FOT temperature showed almost no dependence on the quality of the crystal. It was the value of H_{pk} and T_c that, at least phenomenologically, determined the phase diagram, as shown below. A detailed discussion about the relation between the crystal quality and the temperature dependence of resistivity in the mixed state will be made in a separate paper.[28]

In Fig. 5 the temperature dependence of the FOT field (the FOT line) of some of the crystals are plotted in the H-T diagram as a function of the reduced temperature. As clearly shown in this figure, the FOT line systematically shifts to higher fields as the carrier concentration increases. It is well known that the anisotropy reduces with increasing the carrier concentration.[14] Therefore, Fig. 5 means that the transition field is higher for less anisotropic crystals when compared at the same reduced temperature. This tendency is also valid for crystals OV1–OV5, despite the small difference in the anisotropy as inferred from the values of T_c and H_{pk}. Furthermore, this result is also physically reasonable, because when the electromagnetic anisotropy becomes smaller, fluctuation will be suppressed, and the FOT field should become closer to the upper critical field of the mean field theory. In fact, the reported data of magnetization measurements agree with this picture,[11,15,16] and the theoretical prediction is consistent as well.[29]

IV. DISCUSSION

Two theories have been proposed to account for the FOT; the vortex lattice melting theory and the decoupling theory. The relation between the transition temperature and the field was theoretically derived and can be found in the literature for both theories. In the vortex lattice melting theory,[1] the phase transition temperature (T_m) is given by

$$k_B T_m = \frac{c_L^2 \Phi_0^{5/2}}{4\pi^2 \lambda^2 \sqrt{B}}. \tag{2}$$

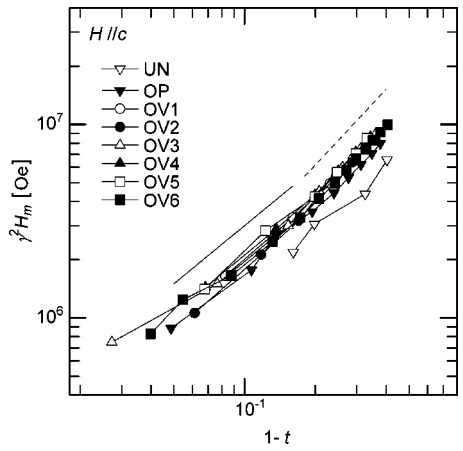

FIG. 6. A trial plot of the FOT fields multiplied by γ^2 as a function of $1-t$ in logarithmic scales. If we suppose $\gamma^2 H_m \propto (1-t)^{\alpha}$, the fitted values of α are 1.4 in the low-temperature high-field region and 1.0 in the high-temperature low-field region, respectively. The solid and dotted lines correspond to $\alpha=1.0$ and $\alpha=1.4$, respectively, which are plotted for guides to the eye.

Here k_B is the Boltzmann constant and c_L the Lindemann number. Adopting the two-fluid model for the temperature dependence of λ $[\lambda^{-2} \propto (1-t)]$, Houghton *et al.*[1] have shown that the melting line obeys the following equation with $\alpha=2$:

$$H_m \propto (1-t)^{\alpha}. \tag{3}$$

However, we found that Eq. (3) with a constant value of α for the whole temperature range does not describe our experimental data well enough, as is obvious from Fig. 6. The high-field low-temperature region is at best fitted with $\alpha=1.4$, while the low-field high-temperature region with $\alpha=1.0$. If we force Eq. (3) to fit the whole temperature range, the fit results in $\alpha=1.1$. The value of 1.4 obtained for the low-temperature region is close to that reported by Zeldov *et al.*[5]

Next, our experimental results are compared with the decoupling theory.[3] In this theory, the temperature dependence of the transition field is expressed as follows:

$$B_D = \frac{2\Phi_0^3}{\pi e T s \lambda^2 \gamma^2}, \tag{4}$$

where e indicates the natural logarithm basis. Using the two-fluid model here yields

$$\gamma^2 H_D \propto \left(\frac{1}{t}-1\right)^m, \tag{5}$$

with $m=1$. Figure 7(a) is a trial plot of $\gamma^2 H_D$ vs $(t^{-1}-1)$ in logarithmic scales. The agreement between experiment and theory is better as compared to the melting theory. However, there are still some deviations from Eq. (5) in the experimental results.

It should be noted here that the two-fluid expression of $\lambda^{-2} \propto (T_c - T)$ used in the derivations of Eqs. (3) and (5) is valid only in the vicinity of T_c. Furthermore, T_m at the left-hand side of Eq. (2) was approximated by T_c in the transformation that yielded Eq. (3). As is evident from Fig. 5, the FOT of Bi2212 is not only observed around T_c but also at much lower temperature, down to about 0.6 times T_c. Therefore, the approximations used in the theories are probably not appropriate for describing the FOT of Bi2212.

To proceed with our discussion, it is necessary to assume a better functional form for the temperature dependence of λ. Shibauchi *et al.*[30] reported that the temperature dependence of λ below 30 K depends strongly on the doping state in Bi2212 single crystals, and argued that this is caused by the difference in the quasiparticle excitation spectrum. On the other hand, at higher temperatures, the region where the FOT

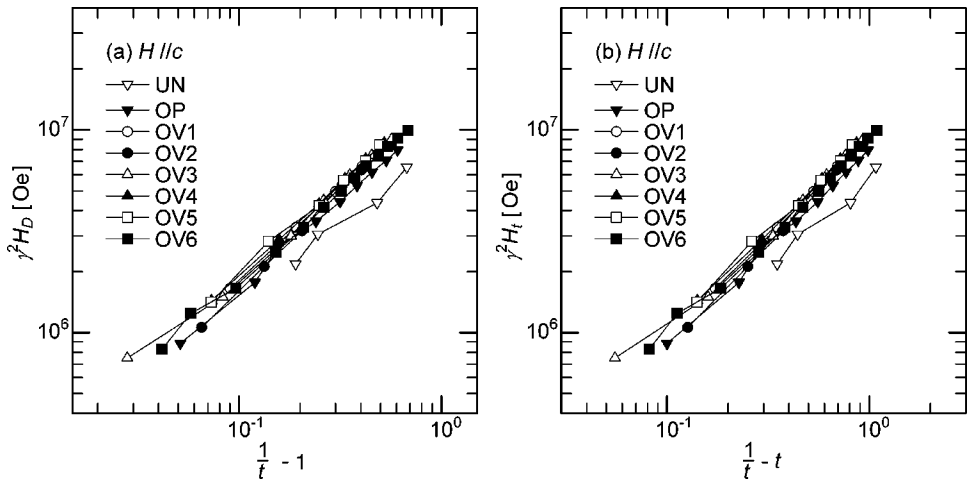

FIG. 7. (a) A trial plot of the FOT fields multiplied by γ^2 as a function of $t^{-1}-1$ in logarithmic scales. If we suppose $\gamma^2 H_D \propto (t^{-1}-1)^m$, the fitted values of m are 0.82, 0.87, 0.91, 0.93, 0.92, 0.92, 0.92, and 0.91 for crystals UN, OP, and OV1–OV6, respectively, and the average is 0.9. (b) A trial plot of the FOT fields multiplied by γ^2 as a function of $t^{-1}-t$ in logarithmic scales. A good linear relation was found between the two quantities. Fitting the data to $\gamma^2 H_t \propto (t^{-1}-t)^n$ resulted in $n=$ 0.93, 0.97, 1.01, 1.04, 1.02, 1.02, 1.02, and 1.03 for crystals UN, OP, and OV1–OV6, respectively, and the average is 1.0.

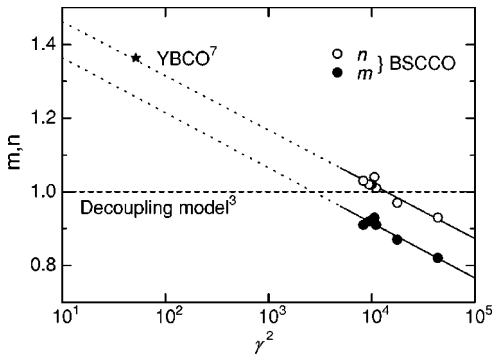

FIG. 8. The exponents m and n of Eqs. (5) and (7), respectively, as a function of γ^2. The broken line is the exponent for the decoupling model (Ref. 3). The star symbol is the α value reported for YBCO (Ref. 7).

takes place, the temperature dependence of λ is rather independent of the doping state.[30] Furthermore, the λ-T curve of Bi2212 at high temperature behaves quite similarly to that of YBCO,[31] for which the following empirical relation was reported to hold:[18]

$$\lambda(t)^{-2} \propto (1-t^2). \tag{6}$$

If we use Eq. (6), we obtain

$$\gamma^2 H_t \propto \left(\frac{1}{t}-t\right)^n, \tag{7}$$

with $n=2$ for the melting theory [Eq. (2)] and $n=1$ for the decoupling theory [Eq. (4)]. Figure 7(b) is a plot of $\gamma^2 H_t$ as a function of $(t^{-1}-t)$ in logarithmic scales. Fitting Eq. (7) to the experimental data resulted to a value close to $n=1$. The analysis using either Eq. (5) or Eq. (7) is summarized as a function of γ^2 in Fig. 8. Clearly, the experimental results are better described by Eq. (7).

The still remaining small deviation in Fig. 8 from $n=1$ might be an indication that a more realistic temperature dependence of λ should be adopted rather than the empirical one, Eq. (6). However, it is also interesting to extrapolate the data shown in Fig. 8 and compare it with YBCO. Welp *et al.* fitted Eq. (3) to their experimental results of YBCO and reported $\alpha=1.36$.[7] Because the FOT takes place only in the vicinity of T_c in YBCO, the difference between Eqs. (3) and (7) should be small, and we think that if the data of YBCO had been fitted to Eq. (7), the exponent n should be similar to the reported value of α, 1.36. This value is surprisingly close to the extrapolation of the data shown in Fig. 8. If we draw a straight line through the data points in Fig. 8 and extend it to $\gamma^2=50$, which corresponds to YBCO, we find $n=1.36$ (open dots) or $m=1.26$ (closed dots).[32] The coincidence between the extrapolated value of n and the exponent reported for YBCO suggests that the exponent might be scaled universally by the anisotropy factor γ.

As has been discussed so far, the decoupling theory describes the observed temperature dependence of the FOT quite well. Nevertheless, we believe that the nature of the FOT is not a pure decoupling transition but melting takes place simultaneously, i.e., it is a sublimation of the flux line lattice, at least in Bi2212. The reasons for this are that no experimental evidence of two separate phase transitions have been reported besides very limited exceptions,[13] and that the change of the entropy associated with the FOT is too large to be accounted for by a single phase transition in Bi2212.[5] The results of a simulation study[33] also supports that decoupling and melting occur simultaneously for a highly anisotropic vortex system like Bi2212, accompanied with a large entropy change at the phase transition.

The question then is why the observed temperature dependence follows well the prediction of the decoupling theory, although the transition is a simultaneous one. This may be related to the above-mentioned scaling behavior of the temperature exponent, and might be explained as follows. In Bi2212, the sublimation is triggered by the breakdown of the phase coherence along the field direction, and therefore, the temperature dependence follows that of the decoupling transition. On the other hand, the coupling of the pancake vortices along the field direction is much stronger in YBCO, and the loss of the crystalline order of the flux line lattice plays a more important role in triggering the FOT, resulting in a temperature dependence that deviates from the prediction of the decoupling theory. We think that the possible scaling behavior of the temperature exponent pointed out in this work and its relation to the nature of the FOT deserve theoretical considerations.

V. CONCLUSIONS

The first-order phase transition of the vortex system under magnetic field was investigated by measuring the in-plane resistivity of Bi2212 single crystals with widely changing the carrier concentration. The transition field at the same reduced temperature increased with the carrier concentration. This tendency was consistent with the results obtained by magnetization studies.[15,16] The transition temperature was rather insensitive to the quality of the crystal. The temperature dependence of the transition field is well described by $H_t \propto (t^{-1}-t)$, independent of the doping state. This formula was derived from the decoupling theory by assuming the empirically found temperature dependence of λ rather than the expression of the two-fluid model. Finally, we pointed out the possibility that the exponent of the temperature dependence of the phase transition field is scaled by the anisotropy of the system.

ACKNOWLEDGMENTS

The present study was supported, in part, by the Core Research for Evolutional Science and Technology (CREST) Program of the Japan Science and Technology Corporation (JST), and by the Tokyo-Ohka foundation.

*Corresponding author. Present address: Institute of Inorganic Synthesis, Yamanashi University, Miyamae 7, Kofu-city, Yamanashi 400-8511, Japan.

†Present address: Center for Integrated Research in Science and Engineering, Nagoya University, Furo-cho, Chikusa-ku, Nagoya 464-8603, Japan.

[1] D.R. Nelson, Phys. Rev. Lett. **60**, 1973 (1988); A. Houghton, R.A. Pelcovits, and A. Sudbø, Phys. Rev. B **40**, 6763 (1989).

[2] M.P.A. Fisher, Phys. Rev. Lett. **62**, 1415 (1989); D.S. Fisher, M.P.A. Fisher, and D.A. Huse, Phys. Rev. B **43**, 130 (1991).

[3] L.I. Glazman and A.E. Koshelev, Phys. Rev. B **43**, 2835 (1991); L.L. Daemen, L.N. Bulaevskii, M.P. Maley, and J.Y. Coulter, Phys. Rev. Lett. **70**, 1167 (1993); L.L. Daemen, L.N. Bulaevskii, M.P. Maley, and J.Y. Coulter, Phys. Rev. B **47**, 11 291 (1993); R. Ikeda, J. Phys. Soc. Jpn. **64**, 1683 (1995).

[4] H. Safar, P.L. Gammel, D.A. Huse, and D.J. Bishop, Phys. Rev. Lett. **69**, 824 (1992); W.K. Kwok, S. Fleshler, U. Welp, V.M. Vinokur, J. Downey, and G.W. Crabtree, *ibid.* **69**, 3370 (1992).

[5] E. Zeldov, D. Majer, M. Konczykowski, V.B. Geshkenbein, V.M. Vinokur, and Shtrikman, Nature (London) **375**, 373 (1995).

[6] R. Liang, D.A. Bonn, and W.N. Hardy, Phys. Rev. Lett. **76**, 835 (1996); T. Nishizaki, Y. Onodera, N. Kobayashi, H. Asaoka, and H. Takei, Phys. Rev. B **53**, 82 (1996).

[7] U. Welp, J.A. Fendrich, W.K. Kwok, G.W. Crabtree, and B.W. Veal, Phys. Rev. Lett. **76**, 4809 (1996).

[8] S. Watauchi, H. Ikuta, J. Shimoyama, and K. Kishio, Physica C **259**, 373 (1996).

[9] A. Schilling, R.A. Fisher, N.E. Phillips, U. Welp, D. Dasgupta, W.K. Kwok, and G.W. Crabtree, Nature (London) **382**, 791 (1996); A. Junod, M. Roulin, J. Genoud, B. Revaz, A. Erb, and E. Walker, Physica C **275**, 245 (1997); A. Schilling, R.A. Fisher, N.E. Phillips, U. Welp, W.K. Kwok, and G.W. Crabtree, Phys. Rev. Lett. **78**, 4833 (1997).

[10] T. Naito, T. Nishizaki, F. Matsuoka, H. Iwasaki, and N. Kobayashi, Czech. J. Phys. **46**, 1585 (1996).

[11] T. Sasagawa, K. Kishio, Y. Togawa, J. Shimoyama, and K. Kitazawa, Phys. Rev. Lett. **80**, 4297 (1998); T. Sasagawa, Y. Togawa, J. Shimoyama, A. Kapitulnik, K. Kitazawa, and K. Kishio, Phys. Rev. B **61**, 1610 (2000).

[12] D.T. Fuchs, R.A. Doyle, E. Zeldov, D. Majer, W.S. Seow, R.J. Drost, T. Tamegai, S. Ooi, M. Konczykowski, and P.H. Kes, Phys. Rev. B **55**, R6156 (1997).

[13] C.D. Keener, M.L. Trawick, S.M. Ammirata, S.E. Hebboul, and J.C. Garland, Phys. Rev. Lett. **78**, 1118 (1997).

[14] Y. Kotaka, T. Kimura, H. Ikuta, J. Shimoyama, K. Kitazawa, K. Yamafuji, K. Kishio, and D. Pooke, Physica C **235-240**, 1529 (1994).

[15] T. Hanaguri, T. Tsuboi, A. Maeda, T. Nishizaki, N. Kobayashi, Y. Kotaka, J. Shimoyama, and K. Kishio, Physica C **256**, 111 (1996); B. Khaykovich, E. Zeldov, D. Majer, T.W. Li, P.H. Kes, and M. Konczykowski, Phys. Rev. Lett. **76**, 2555 (1996).

[16] J. Shimoyama, K. Kishio, H. Ikuta, S. Watauchi, M. Okuya, and K. Kitazawa, Physica C **282-287**, 2055 (1997).

[17] T. Tsuboi, T. Hanaguri, and A. Maeda, Phys. Rev. B **55**, R8709 (1997); D.T. Fuchs, E. Zeldov, D. Majer, R.A. Doyle, T. Tamegai, S. Ooi, and M. Konczykowski, *ibid.* **54**, R796 (1996); D.T. Fuchs, E. Zeldov, M. Rappaport, T. Tamegai, S. Ooi, and H. Shtrikman, Nature (London) **391**, 373 (1998).

[18] D.A. Bonn, R. Liang, T.M. Riseman, D.J. Baar, D.C. Morgan, K. Zhang, P. Dosanjh, T.L. Duty, A. MacFarlane, G.D. Morris, J.H. Brewer, W.N. Hardy, C. Kallin, and A.J. Berlinsky, Phys. Rev. B **47**, 11 314 (1993).

[19] N. Motohira, K. Kuwahara, T. Hasegawa, K. Kishio, and K. Kitazawa, J. Ceram. Soc. Jpn. **97**, 994 (1989).

[20] J. Shimoyama, K. Kishio, Y. Kotaka, K. Kitazawa, and K. Yamafuji, Proceedings of the 6th U.S.-Japan Workshop on High-T_c Superconductors (World Scientific, Houston, 1994), p. 245; K. Kishio, J. Shimoyama, Y. Kotaka, and K. Yamafuji, Proceedings of the 7th International Workshop on Critical Currents in Superconductors (World Scientific, Alpbach, 1994), p. 339.

[21] V.M. Vinokur, B. Khaykovich, E. Zeldov, M. Konczykowski, R.A. Doyle, and P.H. Kes, Physica C **295**, 209 (1998).

[22] T. Giamarchi and P. Le Doussal, Phys. Rev. B **55**, 6577 (1997).

[23] B. Horovitz and T. Ruth Goldin, Phys. Rev. Lett. **80**, 1734 (1998).

[24] A.E. Koshelev and V.M. Vinokur, Phys. Rev. B **57**, 8026 (1998).

[25] B. Khaykovich, M. Konczykowski, E. Zeldov, R.A. Doyle, D. Majer, P.H. Kes, and T.W. Li, Phys. Rev. B **56**, R517 (1997).

[26] V.M. Vinokur, P.H. Kes, and A.E. Koshelev, Physica C **168**, 29 (1990).

[27] S. Ooi, T. Shibauchi, and T. Tamegai, Physica C **302**, 339 (1998).

[28] H. Kobayashi *et al.* (unpublished).

[29] M. Tinkham, *Introduction to Superconductivity (Second Edition)* (McGraw-Hill Inc., Singapore, 1996).

[30] T. Shibauchi, N. Katase, T. Tamegai, and K. Uchinokura, Physica C **264**, 227 (1996).

[31] T. Shibauchi (private communication).

[32] The fits through the data points give $m = 1.51 - 6.50 \times 10^{-2} \ln \gamma^2$ and $n = 1.61 - 6.40 \times 10^{-2} \ln \gamma^2$.

[33] N.K. Wilkin and H. Jeldtoft Jensen, Europhys. Lett. **40**, 423 (1997).